

Synthesis of Silica Membranes on a Porous Stainless Steel by Sol-Gel Method and Effect of Preparation Conditions on Their Permselectivity

Dong-Wook Lee,^{†,‡} Seung-Eun Nam,[†] Bongkuk Sea,[†] Son-Ki Ihm,[‡] and Kew-Ho Lee^{†,*}

[†]Membrane and Separation Research Center, Korea Research Institute of Chemical Technology,
P.O. Box 107, Yuseong, Daejeon 305-606, Korea

[‡]Department of Chemical and Biomolecular Engineering, National Research Laboratory for Environmental Catalysis,
Korea Advanced Institute of Science and Technology, 373-1 Guseong-dong, Yuseong-gu, Daejeon 305-701, Korea
Received February 25, 2004

A porous stainless steel (SUS) as a substrate of silica composite membranes for hydrogen purification was used to improve mechanical strength of the membranes for industrial application. The SUS support was successfully modified by using submicron Ni powder, SiO₂ sols with particle size of 500 nm and 150 nm in turns. Silica top layer was coated on the modified supports under various preparation conditions such as calcination temperature, dipping time and repeating number of dipping-drying process. The calcination temperature for proper sintering was between H ttig temperature and Tamman temperature of the coating materials. Maximum hydrogen selectivity was investigated by changing dipping time. As repeating number of dipping-drying process increased, permeances of nitrogen and hydrogen were decreased and H₂/N₂ selectivity was increased due to the reduction of non-selective pinholes and mesopores. For the silica membrane prepared under optimized conditions, permeance of hydrogen was about $3 \times 10^{-5} \text{ cm}^3 \cdot \text{cm}^{-2} \cdot \text{s}^{-1} \cdot \text{cmHg}^{-1}$ combined with H₂/N₂ selectivity of about 20.

Key Words : Silica composite membrane, Sol-gel method, Hydrogen purification

Introduction

In recent years, silica membranes for gas separation have been studied in several groups. Burggraaf *et al.*^{1,2} prepared microporous silica membranes supported on mesoporous-alumina membranes, and showed activated permeation and molecular sieve-like separation factors in the order of 50-200 for H₂/CH₄. They also prepared alumina-silica membranes for separation of propane and propylene by sol-gel method.³ Brinker *et al.* prepared ultramicroporous (pore radius < 10 Å) separation layers onto commercial alumina supports using dip-coating with polymeric silica sols.⁴ They demonstrated a template approach to prepare microporous inorganic membranes exhibiting high flux combined with high selectivity, overcoming limitations inherent to both conventional inorganic approaches such as sol-gel method and chemical vapor deposition (CVD),⁵ and introduced surfactant-templated silica (STS) intermediate layer to prevent a subsequently deposited microporous overlayer from penetrating into the -alumina support.⁶ Verweij *et al.* synthesized hydrophobic silica membranes using methyl-triethoxy-silane (MTES) and tetra-ethyl-ortho-silicate (TEOS) for application in humid process streams.⁷ They studied the growth of polymeric structure of silica using SAXS,⁸ and prepared silica membranes with micropores of 5 Å using sol-gel synthesis starting from TEOS.⁹ Morooka *et al.* showed that hybridization of silica and polyamic acid were effective to form defect-free thin composite membranes,¹⁰ and the use of phenyltriethoxysilane (PTES) and diphenyl

diethoxysilane (DPDES) was effective in controlling micropore size.¹¹ Gavalas *et al.* used temporary carbon barriers in order to prepare hydrogen-permselective silica membranes supported on porous Vycor support tubes by CVD.¹² Nair *et al.* prepared molecular sieving silica membranes with He/N₂ permselectivity around 1000.¹³

It is well-known that the silica composite membranes are generally fabricated by sol-gel method or CVD, and performance of the CVD silica membrane was better than that of sol-gel silica membranes. However, comparing to CVD, sol-gel method needs a simple apparatus and process, which give rise to suitability for industrial application. In this study, we have prepared the silica composite membranes supported on a porous stainless steel substrate by sol-gel method. While alumina supports generally used for a substrate of inorganic composite membranes are rather brittle and mechanically weak, the porous stainless steel (SUS) gives high mechanical strength and ductility to inorganic composite membranes. The permeation performance of SiO₂/SUS composite membranes has been observed by changing various preparation conditions. In addition, we have studied the effect of each preparation condition on permselectivity of the stainless steel supported silica membrane based on the permeation results and membrane morphology.

Experimental Section

Synthesis of SiO₂ sols. Several silica sols were prepared as materials for modification of porous stainless steel (SUS) supports. Colloidal silica sols with particle size of 500 nm

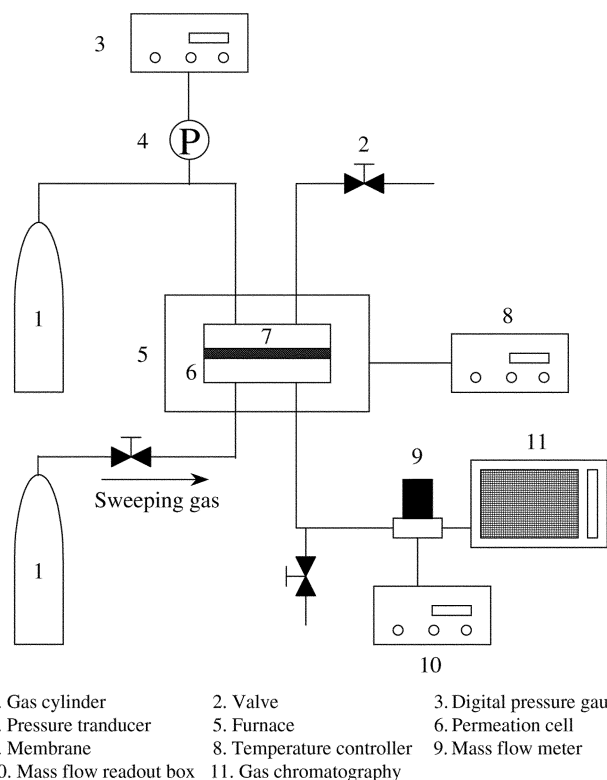
*Corresponding Author. e-mail: khlee@kriect.re.kr

and 150 nm were prepared under base-catalyzed condition via hydrolysis of tetraethyl orthosilicate (TEOS) purchased from Aldrich. For silica sols of 500 nm, concentration of NH_3 and distilled water based on TEOS of 0.28 M were 3.3 M and 10 M, respectively. The volume of reaction mixture was adjusted to 500 mL with ethanol.¹⁴ Prior to the addition of $\text{NH}_3/\text{H}_2\text{O}$ mixture, TEOS/ethanol mixture was stirred vigorously in an oil bath of 50 °C. The addition of the $\text{NH}_3/\text{H}_2\text{O}$ was carried out dropwise followed by refluxing the mixture for 3 h at vigorous stirring resulting in the stable colloidal silica sol.

For silica sol of 150 nm, concentration of NH_3 and distilled water based on TEOS of 0.28 M were 0.6 M and 15 M, respectively. The sol was also synthesized via the same method as the silica sol of 500 nm. Polymeric silica sol for top layer was prepared under acid-catalyzed condition. A molar ratio of TEOS, distilled water and nitric acid was 0.096/0.56/0.008. A mixture of TEOS, distilled water and nitric acid was stirred at room temperature for about 20 min. The reaction mixture was diluted with distilled water to adjust the volume to 500 mL, followed by 8 hr refluxing at 80 °C under vigorous stirring.¹⁵

Modification of porous stainless steel supports. Disks of 316L SUS used as a porous substrate were purchased from Mott Metallurgical. The SUS support has a thickness of 1 mm, a disk area of 5 cm², and an average pore size of 0.5 μm . The support as purchased has wide pore size distribution, rough surface and too many macropores above 10 μm to be used as a support of the composite membrane directly. Some modifications of the porous stainless steel substrate were needed using submicron nickel powder and colloidal silica sols, so that the pore size and surface roughness of the substrate could be gradually reduced. The stainless steel support was modified by rubbing nickel submicron powder on the front side of the support under vacuum of the back side, and calcined under vacuum at 800 °C for 300 min. The Ni modified support was modified again with the colloidal silica sol (500 nm) by dip-coating method, followed by drying overnight and calcination at 650 °C for 2 h.^{16,17} Finally, the support was modified with the colloidal silica sol (150 nm) by dip-coating method under the same conditions of drying and calcination as modification with SiO_2 sol (500 nm).

Optimization of preparation conditions of top layer. The silica composite membranes supported on the modified SUS were prepared with polymeric silica sol changing variations of dip-coating method such as calcination temperature, dipping time and repeating number of dipping-drying process. The dipping time was varied to 30 sec, 60 sec and 90 sec. The dipping-drying process was repeated 2 times, 4 times and 6 times, respectively. The dried membranes were calcined under air for 10 min at 400 °C, 500 °C, 600 °C and 700 °C, respectively. The drying procedure of dip-coated membranes were conducted at 200 °C for 10 min. Ramping rate for drying and calcination was 0.3 °C/min. Optimal conditions of top layer preparation were investigated by changing the variations.



1. Gas cylinder 2. Valve 3. Digital pressure gauge
4. Pressure transducer 5. Furnace 6. Permeation cell
7. Membrane 8. Temperature controller 9. Mass flow meter
10. Mass flow readout box 11. Gas chromatography

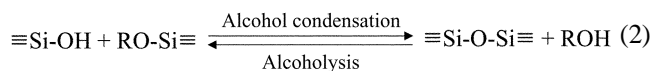
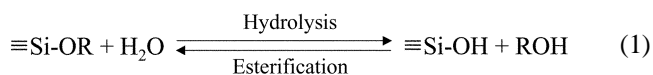
Figure 1. Schematic diagram of the permeation apparatus.

Permeation measurements. Permeation measurements were made with gases of nitrogen and hydrogen at permeation temperature between room temperature and 250 °C. The permeation apparatus is schematically shown in Figure 1. The system consists of a membrane cell, furnace, temperature controller, pressure gauge, pressure transducer and mass flow meter. The transmembrane pressure difference was varied from 2 to 10 psi. Permeation area was 4.52 cm². The selectivity is defined as the ratio of the permeance of hydrogen to that of nitrogen under the same transmembrane pressure difference and temperature.

Characterization. Scanning electron microscopy (SEM, JOEL JSM-840A) was used to characterize the silica composite membranes prepared by changing several conditions. Cross-section and surface of the membrane and particle size of silica sols were observed. For polymeric silica sol, transmission electron microscopy (TEM, EM 912 OMEGA, Carl Zeiss) was used due to measurement limitation of SEM.

Results and Discussion

Characterization of SiO_2 sols and supports. Reactions of TEOS in alcohol as a cosolvent are given below.



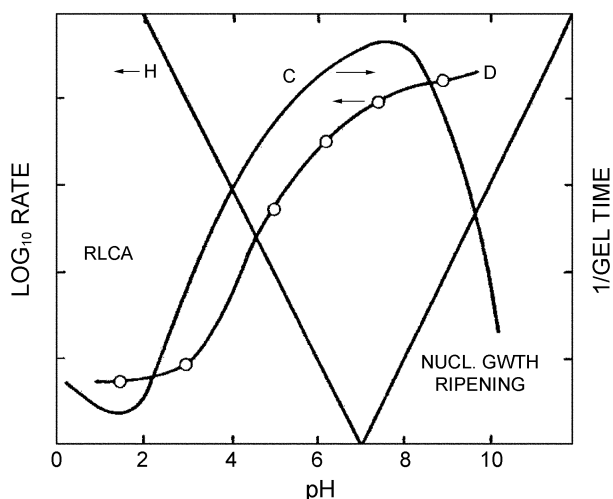
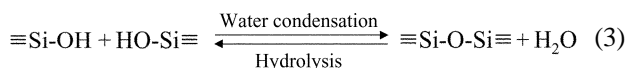


Figure 2. Schematic representation of the pH-dependences of hydrolysis (H), condensation (C) and dissolution (D) [14].



Solubility of silica particles in alcohol solution is proportional to surface curvature of particles. If particle size of silica is more than about 100 nm, reverse reaction of (2) and (3) is not important. But small silica particles are dissolved and provided as a monomer in solution, due to reverse reaction of (2) and (3). As the monomers react with large silica particles, number of silica particles in solution decreases and remaining particle size increases. This phenomenon is called Ostwald ripening. Particles grow continuously until solubility of particles decrease enough, and stable silica sol with average particle size above 100 nm is produced. It was shown in Figure 2 that dissolution become very important under base-catalyzed condition.¹⁴

SEM images of silica sols of 500 and 150 nm are shown in Figure 3. It is revealed that sphere-shaped silica particles above 100 nm was obtained uniformly. The SUS substrate was modified by using Ni powder, SiO₂ sol (500 nm) and SiO₂ sol (150 nm) in turns. SEM image of cross-section of supports in Figure 4 shows that pore size of the SUS support was successfully reduced and surface of the modified SUS support became smoother. Permeation measurement was made in order to estimate performance of the modified support. Figure 5 shows that nitrogen permeance of the modified support decreased with an increase in permeation temperature, and was increased with increasing pressure difference. While the temperature dependence of nitrogen permeance showed Knudsen diffusion characteristics, the pressure dependence of that indicated slight contribution of viscous flow. TEM image of polymeric silica sol prepared as a coating material of top layer is shown in Figure 6. Particle size of polymeric sol is about 1.5 nm.

Effect of calcination temperature on top layer. It is well-known that calcination temperature significantly affects morphology and permeation performance of the inorganic composite membranes. Sintering during calcination process

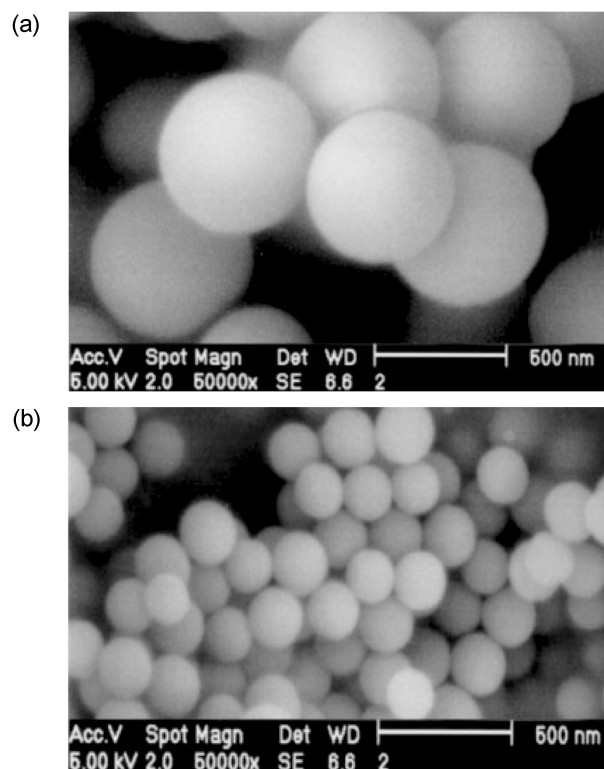


Figure 3. SEM images of (a) SiO₂ sol (500 nm) and (b) SiO₂ sol (150 nm).



Figure 4. SEM image of cross-section of the SiO₂(150 nm)/SiO₂(500 nm)/Ni-SUS support.

is a process of densification driven by interfacial energy. Materials move by viscous flow or diffusion in such a way as to eliminate porosity and thereby reduce the solid-vapor interfacial area. In this study, calcination temperature was varied to 400 °C, 500 °C, 600 °C and 700 °C. Dipping time and repeating number of dipping-drying process were fixed at 90 sec and 4 times, respectively. SEM images of the silica composite membranes prepared by changing calcination temperature are shown in Figure 7. In case of the silica composite membranes calcined at 400 °C and 500 °C, morphology of the top layer is relatively smooth and dense. However, at 600 °C, the coating layer started being collapsed. Finally the top layer was totally collapsed and

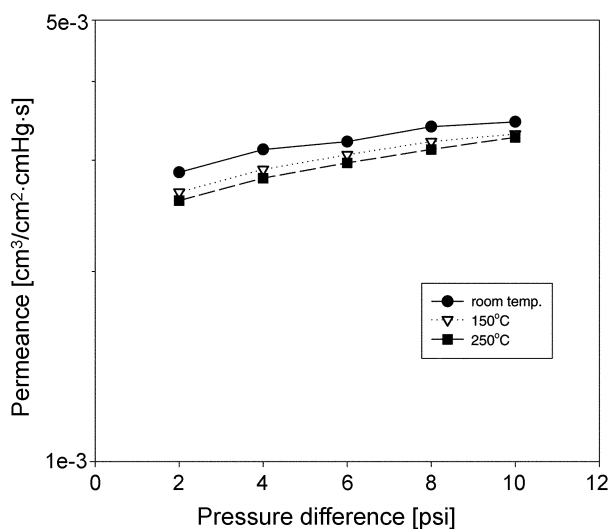


Figure 5. N₂ permeance of the SiO₂(150 nm)/SiO₂(500 nm)/Ni-SUS support.

surface of the SUS support appeared after calcination at 700 °C. The results are due to calcination temperature, ramping rate and atmosphere of calcination (under air or vacuum). The objectives of calcination are to fire impurity included in the membrane, to give mechanical strength to the coating layer and to produce micropores of the membrane through proper sintering. If calcination temperature is too high, the skin layer is collapsed and formation of the effective pores

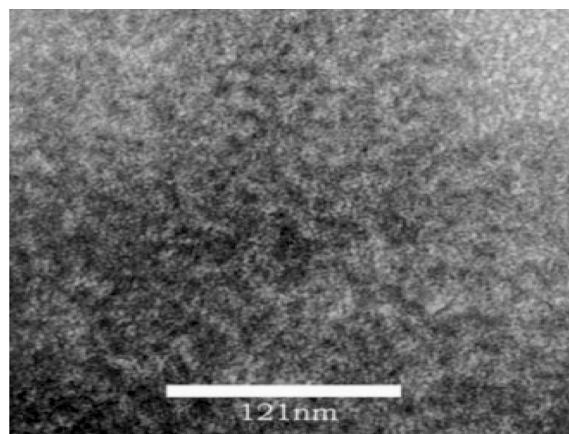
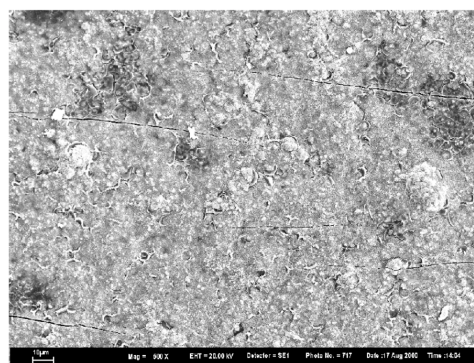


Figure 6. TEM image of the polymeric silica sol.

cannot be expected by excessive sintering. As shown in Figure 7, high calcination temperature above 600 °C led to undesirable morphology of membrane surface and permeation performance due to excessive sintering. In general, surface atoms of inorganic materials start moving at H ttig temperature which is 0.3 times melting point, and lattice of bulk moves at Tamman temperature which is 0.5 times melting point. Melting point of silica and nickel are 1710 °C and 1452 °C, respectively.¹⁸ H ttig temperature of silica and nickel are 320 °C and 245 °C, and Tamman temperature are 720 °C and 590 °C, respectively. It is confirmed that calcination temperature of 600 °C and 700 °C, at which the



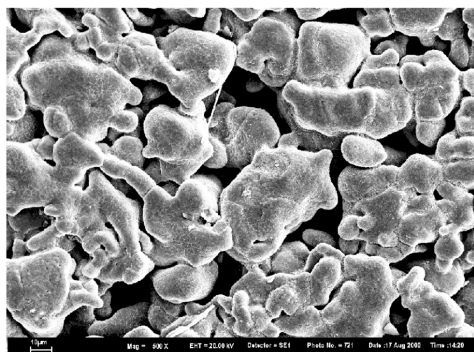
(a)



(b)



(c)



(d)

Figure 7. SEM images of surfaces of the SiO₂ composite membranes prepared at different calcination temperature: (a) 400 °C, (b) 500 °C, (c) 600 °C, (d) 700 °C.

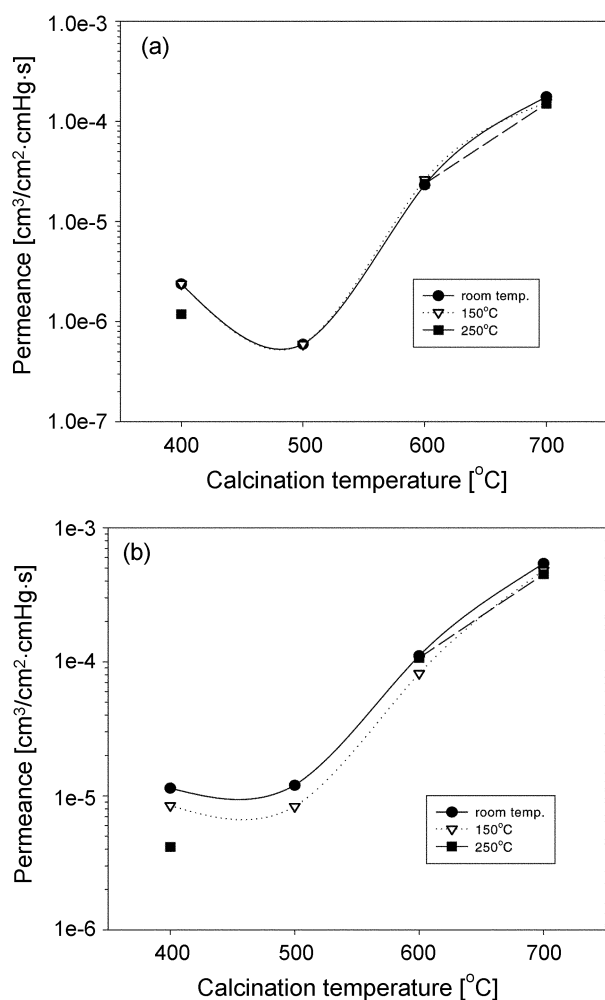


Figure 8. The effect of the calcination temperature on (a) N_2 and (b) H_2 permeances of the SiO_2 composite membranes with different permeation temperature.

skin layer was collapsed, is almost consistent with Tamman temperature of silica and nickel. However, surface of the modified support in Figure 4 was stable, although nickel and SiO_2 (500 nm and 150 nm) on the support was calcined at 800 °C and 650 °C, respectively. Because nickel was calcined under vacuum with ramping rate of 3 °C/min faster than 0.3 °C/min for top layer coating, and SiO_2 (500 nm) and SiO_2 (150 nm) was also calcined with ramping rate of 0.6 °C/min. Calcination under air promotes sintering more than under vacuum, and roughness of membrane surface increases with a decrease in the ramping rate.¹⁹ Therefore the intermediate layers of nickel and colloidal silica on the SUS support were stable during calcination of the support even at 600–800 °C due to fast ramping rate and calcination under vacuum, while they were unstable at calcination temperature of 600 °C under preparation condition of top layer (slow ramping rate and calcination under air). Consequently, it is concluded that high temperature above 600 °C is not suitable to obtain stable silica top layer, because the excessive sintering at high temperature caused a decrease of membrane performance. The effect of the calcination temperature

Table 1. The effect of the calcination temperature on H_2/N_2 selectivity with different permeation temperature

Calcination temperature (°C)	Permeation temperature (°C)		
	room temp.	150 °C	250 °C
400	4.80	3.55	3.50
500	20.20	14.00	–
600	4.77	3.13	4.51
700	3.08	3.12	3.01

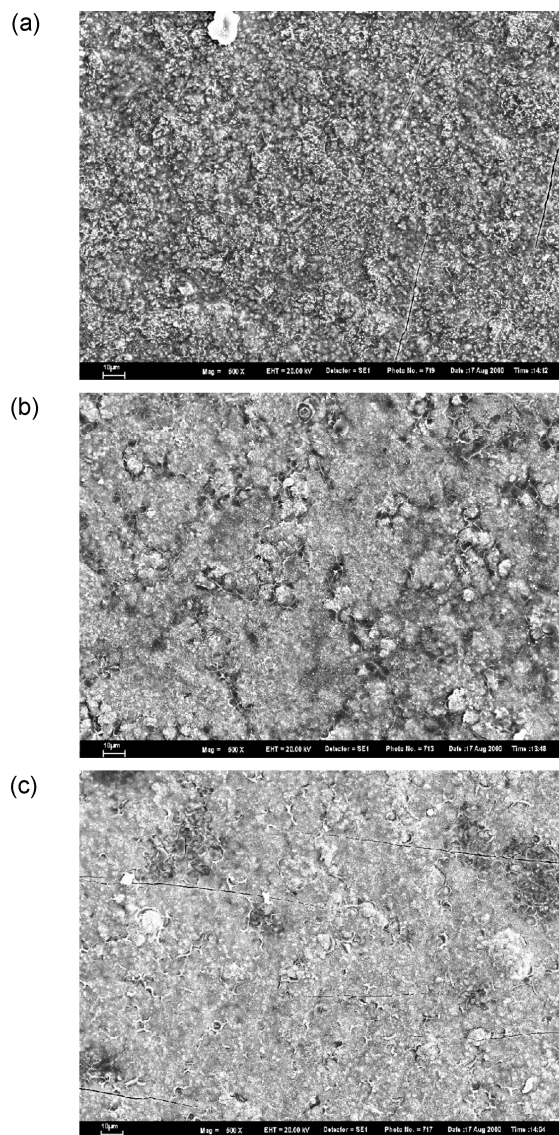


Figure 9. SEM images of surfaces of the SiO_2 composite membranes with different dipping time: (a) 30 sec, (b) 60 sec, (c) 90 sec.

on nitrogen and hydrogen permeances is shown in Figure 8. The permeances were increased rapidly at calcination temperature of 600 °C and 700 °C. When calcination temperature was increased from 400 °C to 500 °C, nitrogen and hydrogen permeances were decreased and constant, respectively. It means that calcination at 500 °C reduced

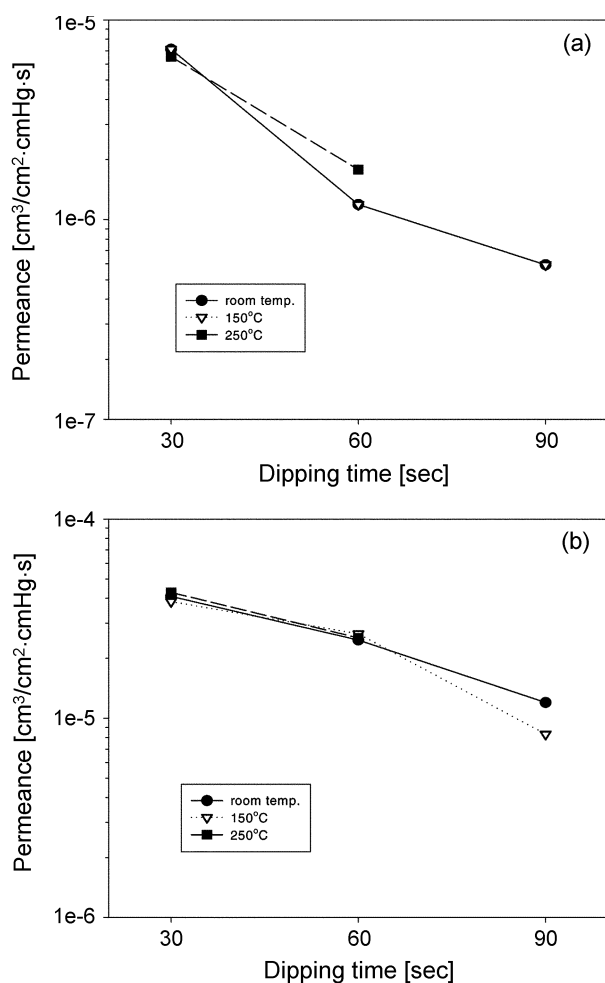


Figure 10. The effect of dipping time on (a) N_2 and (b) H_2 permeances of the SiO_2 composite membranes with different permeation temperature.

relatively large pores through which the nitrogen permeates. The effect of calcination temperature on H_2/N_2 selectivity is given in Table 1. The silica composite membrane calcined at $500\text{ }^\circ\text{C}$ showed the highest H_2/N_2 selectivity. Therefore it is considered that pore size could be controlled by changing the calcination temperature, and hydrogen-selective pores could be produced at the calcination temperature between Httig and Tamman temperature, where proper sintering can be induced.

Effect of dipping time on top layer. Dipping time was varied to 30 sec, 60 sec and 90 sec. Calcination temperature and repeating number of dipping-drying process were fixed at $500\text{ }^\circ\text{C}$ and 4 times, respectively. SEM images of the membrane surfaces with different dipping time are shown in Figure 9. The surface of the silica composite membrane became smoother with an increase in the dipping time, because more silica particles penetrated into the pores of the supports and deposited on the surface of the supports, as contact time between the silica sol and the membrane surface was increased. The effect of dipping time on the permeances of nitrogen and hydrogen is shown in Figure 10. The permeances of nitrogen and hydrogen were decreased

Table 2. The effect of dipping time on the H_2/N_2 selectivity with different permeation temperature

Dipping time (sec)	Permeation temperature ($^\circ\text{C}$)		
	room temp.	150 $^\circ\text{C}$	250 $^\circ\text{C}$
30	5.73	5.40	6.55
60	20.80	22.30	14.20
90	20.20	14.00	–

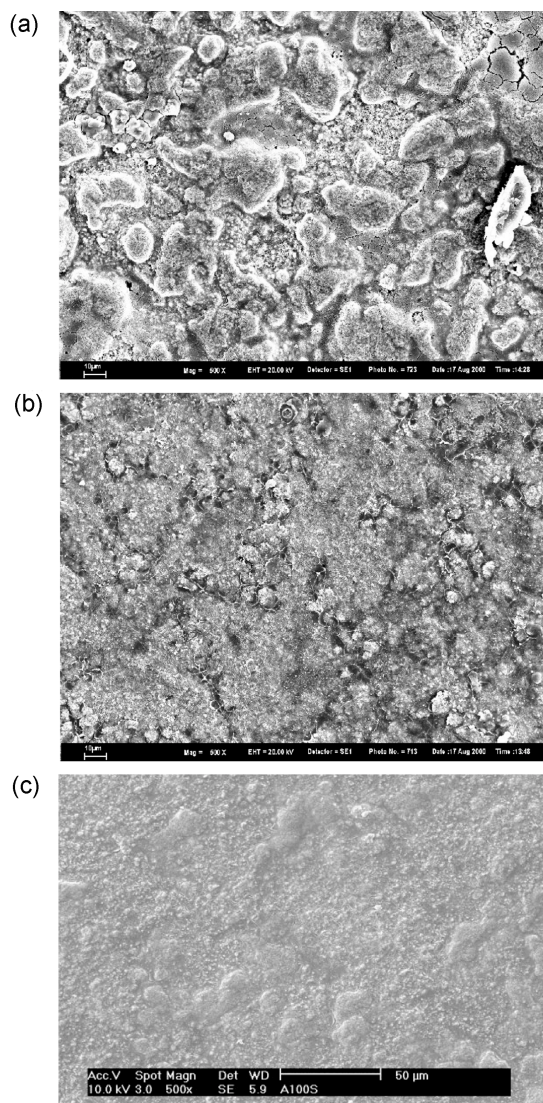


Figure 11. SEM images of surfaces of the SiO_2 composite membranes with different repeating number of dipping-drying process: (a) 2 times, (b) 4 times, (c) 6 times.

with the increase of dipping time. While the permeance of nitrogen decreased rapidly between 30 sec and 60 sec, the hydrogen permeance decreased rapidly between 60 sec and 90 sec. The effect of dipping time on the H_2/N_2 selectivity is shown in Table 2. The H_2/N_2 selectivity was the highest at 60 sec of dipping time and was decreased at 90 sec. Maximum H_2/N_2 selectivity was obtained with the increase in dipping time. It is well-known that, in case of dip-coating method,

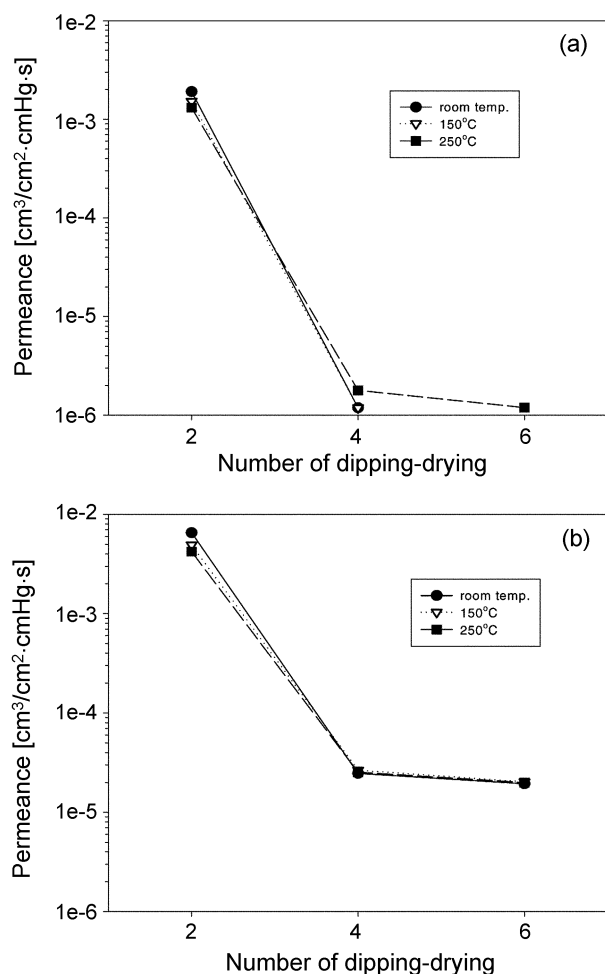


Figure 12. The effect of repeating number of dipping-drying process on (a) N_2 and (b) H_2 permeances of the SiO_2 composite membrane with different permeation temperature.

capillary filtration occurs when the dry support comes into contact with coating solution and the pore surface is wetted by the coating solution, followed by capillary suction of the support. As a result, filtration cake is formed on the surface of the support. Comparing to the membrane prepared at dipping time of 60 sec, the silica composite membrane prepared at dipping time of 90 sec showed the decrease in the H_2/N_2 selectivity due to excessive contact of the membrane surface with the sol, which contributed to crack formation induced by an increase in thickness of the surface gel layer.

Effect of repeating number of dipping-drying process on top layer. In order to observe effect of repeating number of dipping-drying process before calcination, dipping-drying process was repeated 2 times, 4 times and 6 times. Dipping time and calcination temperature were respectively 60 sec and 500 as optimized before. SEM images of the silica membrane surface with different repeating number of dipping-drying process are shown in Figure 11. While the surface of the silica membrane prepared by repeating the dipping-drying procedure twice was rather rough, the membrane surface prepared by repeating the dipping-drying

Table 3. The effect of repeating number of dipping-drying process on the H_2/N_2 selectivity with different permeation temperature

Repeating number of dipping-drying	Permeation temperature ($^{\circ}C$)		
	room temp.	150 $^{\circ}C$	250 $^{\circ}C$
2	3.42	3.24	3.22
4	20.80	22.30	14.20
6	>32.60	>34.00	16.70

process 4 times became smoother and denser. In case of 6 times repeats, the surface of the skin layer was highly dense and smooth. The membrane surface became denser and smoother with increasing the repeating number of the dipping-drying process. Figure 12 shows the effect of repeating number of dipping-drying process on the permeances of nitrogen and hydrogen, and the H_2/N_2 selectivities with different repeating number is shown in Table 3. Between 2 times and 4 times, both of nitrogen and hydrogen permeances were drastically diminished, the H_2/N_2 selectivity was substantially increased. However hydrogen and nitrogen permeances between 4 times and 6 times were decreased a little, the H_2/N_2 selectivity was slightly increased. Based on the results, it can be speculated that pinholes, cracks and mesopores on the silica membrane were gradually reduced with the increase in repeating number of dipping-drying process, because the decrease in the permeance combined with the increase of the selectivity was shown with the increase in repeating number.

Conclusions

The silica composite membranes supported on the porous stainless steel (SUS) supports were successfully prepared by dip-coating method, and effects of preparation conditions on their permselectivity were observed. The top layer of the silica composite membranes was collapsed after calcination at above Tamman temperature of silica and nickel as coating materials. The excessive sintering at above Tamman temperature must be excluded to obtain hydrogen-selective micropores and the formation of micropores via proper sintering of the coating materials can be achieved through calcination at between H ttig temperature and Tamman temperature of the coating materials. Maximum H_2/N_2 selectivity was obtained at dipping time of 60 sec. Comparing to the membrane prepared at dipping time of 60 sec, the silica composite membrane prepared at dipping time of 90 sec showed the decrease in H_2/N_2 selectivity due to excessive contact of the membrane surface with the sol, which contributed to crack formation induced by an increase in thickness of the surface gel layer. As repeating number of dipping-drying process increased, permeances of nitrogen and hydrogen were decreased and H_2/N_2 selectivity was increased due to the reduction of non-selective pinholes and mesopores. In other words, mesopores and pinholes of the membrane was gradually reduced by repeating the dipping-drying procedure.

References

1. De Lange, R. S. A.; Hekkink, J. H. A.; Keizer, K.; Burggraaf, A. J. *J. Membr. Sci.* **1995**, *99*, 57-75.
 2. De Lange, R. S. A.; Hekkink, J. H. A.; Keizer, K.; Burggraaf, A. J. *J. Non-Cryst. Solids* **1995**, *191*, 1-16.
 3. Nair, B. N.; Keizer, K.; Elferink, W. J.; Gilde, M. J.; Verweij, H.; Burggraaf, A. J. *J. Membr. Sci.* **1996**, *116*, 161-169.
 4. Brinker, C. J.; Ward, T. L.; Sehgal, R.; Raman, N. K.; Hietala, S. L.; Smith, D. M.; Hua, D.-W.; Headley, T. J. *J. Membr. Sci.* **1993**, *77*, 165-179.
 5. Raman, N. K.; Brinker, C. J. *J. Membr. Sci.* **1995**, *105*, 273-279.
 6. Tsai, C.-Y.; Tam, S.-Y.; Lu, Y.; Brinker, C. J. *J. Membr. Sci.* **2000**, *169*, 255-268.
 7. De Vos, R. M.; Maier, W. F.; Verweij, H. *J. Membr. Sci.* **1999**, *158*, 277-288.
 8. Nair, B. N.; Elferink, W. J.; Keizer, K.; Verweij, H. *J. Coll. Interf. Sci.* **1996**, *178*, 565-570.
 9. De Vos, R. M.; Verweij, H. *J. Membr. Sci.* **1998**, *143*, 37-51.
 10. Kusakabe, K.; Ichiki, K.; Hayashi, J.-I.; Maeda, H.; Morooka, S. *J. Membr. Sci.* **1996**, *115*, 65-75.
 11. Sea, B.-K.; Kusakabe, K.; Morooka, S. *J. Membr. Sci.* **1997**, *130*, 41-52.
 12. Jiang, S.; Yan, Y.; Gavalas, G. R. *J. Membr. Sci.* **1995**, *103*, 211-218.
 13. Nair, B. N.; Yamaguchi, T.; Okubo, T.; Suematsu, H.; Keizer, K.; Nakao, S.-I. *J. Membr. Sci.* **1997**, *135*, 237-243.
 14. Brinker, C. J.; Scherer, G. W. *Sol-Gel Science; The Physics and Chemistry of Sol-Gel Processing*; Academic Press: New York, 1990.
 15. Naito, M.; Nakahira, K.; Fukuda, Y.; Mori, H.; Tsubaki, J. *J. Membr. Sci.* **1997**, *129*, 263-269.
 16. Lee, D.-W.; Lee, K.-H. *J. Korean Ind. Eng. Chem.* **2001**, *12*, 45-51.
 17. Jun, C.-S.; Lee, K.-H. *J. Membr. Sci.* **1999**, *157*, 107-115.
 18. Perry, R. H.; Green, D. *Perry's Chemical Engineers' Handbook*; McGraw-Hill: New York, 1984.
 19. Simoes, M.; Assis, O. B. G.; Avaca, L. A. *J. Non-Cryst. Solids* **2000**, *273*, 159.
-